Wave-packet approach to noise in multichannel mesoscopic systems

Th. Martin and R. Landauer
IBM Research Division, Thomas J. Watson Research Center, P.O. Box 218, Yorktown Heights, New York 10598
(Received 24 May 1991)

Noise in conductors transmitting electrons coherently between attached reservoirs is calculated by following wave packets incident on the sample. The Pauli principle restricts the occupation of wave packets, spreading electrons more uniformly among the available packets, and thus reducing the noise below that of the classical shot-noise expression for totally uncorrelated electrons. After a brief review of the results for one-dimensional leads, we treat the case of the sample attached to two multichannel leads. A proper choice of basis for the wave packets permits this case to be reduced to that of a set of independent parallel one-channel samples. This picture is extended to the case of excess noise in multiterminal samples at zero temperature, leading to anticorrelated fluctuations between different leads. The anticorrelated fluctuations are analyzed, in particular detail for a Y-shaped three-lead sample. Our wave-packet approach is presented as a physically intuitive alternative to the existing approaches to mesoscopic noise, and leads to identical results.

I. INTRODUCTION

In the past decade, progress in nanostructure fabrication techniques[1] has led to the discovery of many phenomena in mesoscopic physics. Among those are the quantum Hall effect[2] (QHE) and all its derivatives, the quantization of the conductance of a narrow constriction as a function of the gate voltage,[3] the observation of the Aharonov-Bohm effect in metallic rings,[4] etc. In these systems, the reduced size of the samples and a very low temperature can allow electrons to cross the sample in a coherent way. While an electron may suffer elastic collisions with the boundaries of the sample, or with impurities, inelastic collisions, such as phonon scattering, spin-flip, and electron-electron scattering processes, which are responsible for the loss of phase coherence, can be neglected. As a result, interference effects due to the wave nature of the electrons are expected to occur, in close analogy with the propagation of electromagnetic (EM) waves in a complex structure. However, there is one major difference between EM waves and electrons:[5] Electrons obey Fermi-Dirac statistics, while EM waves are composed of photons, obeying Bose-Einstein statistics. For electrons, the Pauli exclusion principle restricts the occupation of quantum-mechanical states, therefore affecting electronic transmission through a sample, while no similar constraint exists for photons: many photons can coexist in the same state. The purpose of this paper is to give an illustration of these effects on excess noise due to electron transport in coherent structures.

To a large extent, the effort in this field has focused on the average properties of electronic transport, such as the conductance. New ways of characterizing these systems include the measurement of the spectral density of current or voltage noise. Here, we will attempt to calculate noise current from quantum-mechanical transmission. As is well understood in classical systems, noise arises whenever random processes are present in electron transport. A classical example is shot noise for vacuum diodes:[6] the uncorrelated emission of electrons from a cathode. In general, noise in solid-state devices can have different origins. First there is $1/f$ noise,[7] which typically arises from fluctuations in the resistance of the sample. Feng, Lee, and Stone[8] showed that the motion of a few defects out of 10^{20} atoms can lead to fluctuations in the conductance of the order $e^2/\hbar$, independent of sample size. On top of the $1/f$ noise, a white spectrum of noise is superposed, associated with the stochastic nature of electron transport. This latter contribution, due to both quantum and thermal fluctuations of the electrons, will be the focus of the present paper. Other sources of noise, such as telegraphic noise[9] due to impurity motion, or the noise associated with the electromagnetic environment which defines the sample, are also present in real systems, but will not be discussed here.

Reference 10 reported measurements of noise in a double-barrier resonant tunneling structure. The measurement frequencies were chose to be small compared to the inverse transit time of an electron through the structure. For frequencies below 100 Hz, $1/f$ noise gave the dominant contribution, but between 1 and 10 kHz the amplitude of the noise signal did not depend on frequency (white noise). For resonant tunneling structures with asymmetric barriers and small transmission, the noise level in that frequency range was found to lie almost at the full shot-noise level. For more highly transmitting symmetric structures, the measured noise was suppressed compared to shot noise.

Another experiment performed by Li *et al.*[11] attempted to measure shot noise in a narrow constriction, at frequencies ranging from 100 Hz to 100 kHz and a temperature of 4.2 K. Upon separation of the spectral density into a $1/f$ and a frequency-independent component, the white-noise contribution was found to increase with the injected current, but never reaching the full level of classical shot noise. The $1/f$ component was attributed to the trapping and detrapping of electrons by impurities. The increase in white noise was attributed to thermal

effects and to the nonadiabaticity of the constriction, which permits the backscattering of electrons incident on the constriction. It was inferred that for an ideal contact (with no backscattering), transport at zero temperature does not generate shot noise, due to the absence of random processes. This conclusion is consistent with the fact that a filled set of states cannot generate any noise, as we shall see below.

At the same time, noise has also been measured in two-dimensional electron systems which exhibit the quantum Hall effect.[12] There, the spectral noise intensity of the longitudinal and Hall voltage was explained in terms of fluctuations in the number of extended states lying in the Landau-level tails. More recently, voltage noise measurements where performed on gated structures,[13] characterizing the noise for fractional and integer filling factors. Noise plateaus were observed for filling factors corresponding to the Hall quantization condition.

Previous calculations of noise in quantum coherent structures have been based on essentially two types of approaches: the wave-packed approach, which was successfully applied to calculate thermal equilibrium noise,[14] or alternatively a first-principles calculation of the current correlations in time,[15–17] which is related to the Keldysh formulation of nonequilibrium quantum statistical mechanics.[18] Much of our work is an attempt to understand and verify the results of Büttiker[17] from the wave-packet viewpoint. Other work,[19] based on semiclassical approaches, has been used to calculate excess noise in small structures, but will not be discussed.

In the wave-packet approach of Ref. 14, electrons are visualized as traveling through the idea leads connected to the sample, forming orthogonal wave packets. Upon hitting the sample, a wave packet may be partially transmitted or reflected, and the fluctuations in current are determined from the occupation probabilities of the different incident states in the leads, as well as the transmissive behavior of the sample.

We pause here, for a supplementary comment on our motivation, and on the relation to the more formal theories.[15–17] The latter invoke the calculation of grand-canonical averages of products of current operators, whose relation to actual noise measurements is not displayed in a direct physical way. First of all, to dispel one possible misperception, current measurements are *not* measurements of momentum. Currents can be measured through their magnetic fields, reflecting the sum of electronic and displacement current, and yielding a result independent of the location along a circuit branch. Most likely, however, they are measurements of voltage across a small resistor inserted between the sample and a reservoir.[20] At the low frequencies of interest in this discussion, low compared to the reciprocal of any kinetic time associated with the sample (see below), noise currents measure the fluctuation in the arrival and departure rate of electrons. In a given time interval, do we have more or less than the average number transmitted into and out of a given lead? That is essentially an electron counting operation; an electron arrives, or does not arrive, and this is relatable to the use of the second quantization formalism in Refs. 15–17. The fluctuations arise from the fact that occupation and transmission probabilities specify an average rate. A given electron, incident on the sample in the form of a wave packet in a given lead, is either transmitted into another lead, or not. Experimentally, of course, it is easier to characterize these fluctuations in the frequency domain, rather than in the time domain, and this is precisely what our analysis addresses.

As mentioned earlier,[21] it is expected that the Pauli exclusion principle will tend to spread electrons apart. Coulomb repulsion between electrons will have a similar effect. In a vacuum diode, such effects have long been known to occur as the voltage between the two electrodes is reduced, and the electron being emitted from the cathode sees both the field due to the applied potential and the field associated with the electron cloud near the cathode. The current is then limited by the applied voltage, and the measured noise lies well below the shot-noise level.[22] While related effects may turn up in mesoscopic systems, we shall not address them, and only consider the independent electron model.

A simplified schematic circuit for noise measurement in a two-terminal structure is illustrated in Fig. 1. The sample to be analyzed is connected on the left- and the right-hand side to two electron reservoirs through ideal leads. Applying a bias between the two reservoirs causes current to flow through the sample. For simplicity, the sample is assumed to be a purely elastic scatterer; inelastic processes take place only in the reservoirs. To permit fluctuating current to flow, the reservoirs are short circuited via two large capacitances. In what follows, the frequency range will be chosen such that (i) the inverse of the typical time associated with an electron passing through the sample (traversal time[23]) is large compared to the measurement frequency, (ii) the impedance of the two capacitors in series is small compared to that of the sample, (iii) the impedance of the stray capacitances due to the electronic circuitry surrounding the sample is large, and (iv) the measurement frequency is low enough to make the self-inductance negligible.

Note that the setup illustrated in Fig. 1 can only be used to measure current noise. To measure voltage fluctuations, which are eliminated by the two large capacitances, we need to disconnect this short circuit and. instead, connect the reservoirs to each other through a higher impedance circuit. The open circuit voltage fluctuations can be calculated from the current fluctuations by simply multiplying the latter quantity by the square of

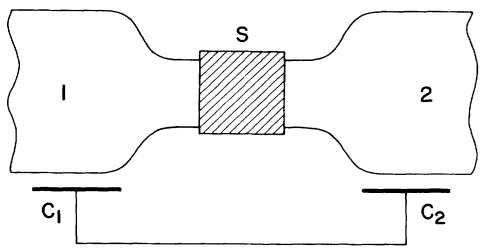

FIG. 1. Transport through a sample connecting two reservoirs at differing chemical potentials. The capacitors provide an effective short circuit at the frequencies of interest.

the resistance of the sample.

The paper is organized in the following way. Section II gives the general definitions and introduces our wave-packet approach in the one-dimensional case, where we obtain explicit formulas for combined thermal and excess noise. Section III is devoted to the multichannel two-terminal case. Section IV deals with the multiterminal case at zero temperature. Section V discusses current correlations in a Y-shaped structure, where effects associated with the Fermi statistics of the electrons are expected. Section VI discusses coherence between leads. The results are summarized in Sec. VII.

II. NOISE IN TWO-TERMINAL STRUCTURES

A. Preliminaries

To illustrate our approach, we first consider the simplest case, where the leads carry only one channel (one-dimensional case). This amounts to saying that electrons traveling in the sample in the form of wave packets are sent from a given lead one at a time, at a rate $1/\tau$, towards the sample region.

If we restrict the wave packets to an energy range ΔE, we can construct a series of successive orthonormal wave packets in the following way:[14,24]

$$\psi^{(n)}(z,t)=\int_{E-\Delta E}^{E+\Delta E}dE'\frac{1}{\Delta E}\left[\frac{1}{2\pi}\frac{dk}{dE'}\right]^{1/2} \times e^{ik(E')z-iE'(t+n\tau)/\hbar}, \tag{2.1}$$

with $\tau=2\pi\hbar/\Delta E$. These wave packets provide a complete basis for waves within ΔE incident from one side; the left side as written in Eq. (2.1). A wave packet is constructed from a superposition of plane waves, each plane wave carrying the same flux, and can be occupied by two electrons, with their respective spins pointing in opposite directions.

The spectral density of current noise $W(\nu)$ in the frequency interval $[\nu,\nu+\delta\nu]$ is obtained from the Fourier transform of the current-current correlation function $C(\tau)$:[25]

$$W(\nu)=4\int_0^\infty d\tau\, C(\tau)\cos(2\pi\nu\tau), \tag{2.2}$$

with

$$C(\tau)=\lim_{T\to\infty}\left[\frac{1}{T}\int_0^T dt\, I(t)I(t+\tau)\right]. \tag{2.3}$$

Using the Fourier transform of the current $I(2\pi\nu)$, the expression for the spectral density of noise becomes

$$W(\nu)=\lim_{T\to\infty}\left[\frac{2}{T}\langle|I(2\pi\nu)|^2\rangle\right], \tag{2.4}$$

where the angular brackets denote an average over pulse histories.

Denoting the current associated with one electron wave packet by $j(t)$, the total current, as a superposition of orthogonal wave packets shifted in time, will then be

$$I(t)=\sum_n j(t-n\tau)g_n, \tag{2.5}$$

where g_n denotes the number (and sign) of the electrons transferred across the sample in the nth pulse period. g_n can take the value $+1$ if a pulse is transmitted to the right, 0 if no pulse is transmitted, or -1 for a pulse transmitted to the left. From Eq. (2.5), the Fourier component of the current reads

$$I(2\pi\nu)=\sum_n g_n j(2\pi\nu)e^{i2\pi\nu n\tau}. \tag{2.6}$$

Because the frequency is assumed to be small compared to the duration of a current pulse, $j(2\pi\nu)$ is essentially an integral over time, of the pulse, and thus reduces to the electric charge e within our framework. The quantity of interest in Eq. (2.4) is then

$$\langle|I(2\pi\nu)^2|\rangle=e^2\sum_{m,n}\langle g_m g_n\rangle\exp[i2\pi\nu\tau(m-n)] =e^2\sum_n\langle g_n^2\rangle. \tag{2.7}$$

The cross terms in Eq. (2.7) vanish after ensemble averaging (or after considering many such terms) because there is no correlation between current pulses in different time slots. The summation over n extends over all T/τ time slots, with each time slot allowing for two electrons with opposite spin. The final right-hand side of Eq. (2.7) is essentially an evaluation of the average value of $\langle g_n^2\rangle$; additionally, the sum depends on the number of terms in the interval T. Therefore, Eq. (2.7) leads to the noise power

$$\langle|[I(2\pi\nu)]^2|\rangle=\frac{Te^2\Delta E}{\pi\hbar}\langle g^2\rangle, \tag{2.8}$$

where we made use of the definition of τ, as required by the orthogonality condition of successive wave packets in Eq. (2.1). Our calculation of the spectral density of noise is, therefore, directly related to the statistics of the current pulses: "Has an electron crossed the sample, and with what probability?"

In the typical situation of interest, a bias is applied between the two reservoirs, and a dc current flows in the sample. To calculate the effect of the bias on the spectral density of noise, we make the substitution $I(t)\to I(t)-\langle I\rangle$ in Eqs. (2.2)–(2.4) and obtain the noise-power contribution for the frequency interval $[\nu,\nu+\delta\nu]$, due to carriers in the energy interval $[E-\Delta E/2,E+\Delta E/2]$:

$$\langle(\Delta I)^2\rangle_{\delta\nu}=\frac{2\,\delta\nu\,\Delta E\,e^2}{\pi\hbar}\langle g^2-\langle g\rangle^2\rangle. \tag{2.9}$$

This is the starting point of our approach. The remaining sections will be devoted to the computation of the fluctuations in occupation probabilities.

B. Excess noise in one dimension

For a two-terminal sample which is narrow enough to allow only one channel, the situation is fairly simple: carriers can be emitted from the right- and left-hand side (Fig. 1). Furthermore, we assume that the wave packets incident from the right and from the left are synchronized. This ensures that a transmitted wave packet from

the left maps into the same state as a reflected wave packet from the right. The reservoirs are assumed to be in thermal equilibrium, with respective occupation probabilities specified by Fermi distribution functions f_1 and f_2 corresponding to chemical potential μ_1 and μ_2, respectively.

There are six possible pulse histories. They are as follows.

(i) The probability for a wave packet incident from the left and the right at the same time is $f_1 f_2$; in this case, no current results.

(ii) The probability that both wave packets are empty is $(1-f_1)(1-f_2)$; again, no current is associated with this case.

(iii) A current $+1$ is measured when a wave packet incident from the left is transmitted to an empty state on the right. The weight factor for this case is $f_1(1-f_2)T$, with T the transmission probability.

(iv) A current -1 is measured when a wave packet incident from the right is transmitted to the left, with probability $f_2(1-f_1)T$ (the probability for transmission to the right is the same as the probability for transmission to the left).

(v) Same as (iii), except that the wave packet is reflected; no current results, and the weight factor is $f_1(1-f_2)(1-T)$.

(vi) Same as (iv), except that the wave packet is reflected; this yields $f_2(1-f_1)(1-T)$. In cases (i), (ii), (v), and (vi), the deviation from the average over the set of pulses is $-T(f_1-f_2)$ (we have chosen the positive sign for carrier motion from left to right). For case (iii) this deviation is $1-T(f_1-f_2)$ and for case (iv) the deviation is $1+T(f_1-f_2)$.

The expression for $\langle g^2-\langle g\rangle^2\rangle$ is thus the sum of each mean-square deviation, multiplied by its appropriate weight factor. The result is

$$\begin{aligned}\langle g^2-\langle g\rangle^2\rangle &= T(f_1+f_2-2f_1f_2)-(f_1-f_2)^2T^2 \\ &= 2Tf_2(1-f_1) \\ &\quad +T(f_1-f_2)[1-T(f_1-f_2)] \ . \end{aligned} \tag{2.10}$$

The total excess noise is obtained by inserting (2.9) into (2.10) and then adding up each contribution of the form Eq. (2.9) over all energy intervals $[E-\Delta E/2, E+\Delta E/2]$. We then find

$$\begin{aligned}\langle(\Delta I)^2\rangle_{\delta\nu} &= \frac{4e^2\delta\nu}{\pi\hbar}\int dE\ T(E)f_2(1-f_1) \\ &\quad +\frac{2e^2\delta\nu}{\pi\hbar}\int dE\ T(E)(f_1-f_2) \\ &\quad \times[1-T(E)(f_1-f_2)] \ . \end{aligned} \tag{2.11}$$

This expression can be written in a more transparent way if we consider the special case where the transmission coefficient has a weak dependence on the energy $T(dT/dE)^{-1} \gg \mu_1-\mu_2, k_B\Theta$ (we set $\mu_1>\mu_2$), which corresponds to the limit of low temperatures and small applied biases. In that case we can take $T(E)$ to be constant within the range of integration in Eq. (2.11) that matters. This simplification is *not* crucial, but only serves to yield more transparent results.

In the low-temperature limit, $k_B\Theta \ll \mu_1-\mu_2$, the first contribution in Eq. (2.11) vanishes, as the two factors $(1-f_1)$ and f_2 have no nonvanishing region of overlap. The second term of this equation gives a contribution

$$\lim_{\Theta\to 0}\langle(\Delta I)^2\rangle_{\delta\nu} = \frac{2e^2\delta\nu}{\pi\hbar}T(1-T)(\mu_1-\mu_2) \ . \tag{2.12}$$

In the limit of small transmission ($T\to 0$), we recover the classical shot-noise formula. It is interesting to note that the noise is suppressed in the limit of perfect transmission ($T\to 1$): there is a symmetry between this case and that of weak transmission. A channel which cannot transmit generates no noise, and so does a perfectly transmissive channel. In terms of the average current, we can rewrite the zero-temperature result of Eq. (2.12) in the form

$$\lim_{\Theta\to 0}\langle(\Delta I)^2\rangle_{\delta\nu} = 2e\,\delta\nu\langle I\rangle(1-T) \ . \tag{2.13}$$

Apart from the factor $(1-T)$, this is the shot-noise formula. This states that excess noise in a quantum system is always less than the shot-noise level, precisely as observed in the experiments discussed in the Introduction.

In the opposite limit, $k_B\Theta \gg \mu_1-\mu_2$, where the temperature is large compared to the applied bias, we should recover the expression for thermal equilibrium noise. This time, only the first term on the right-hand side of Eq. (2.11) survives, and we find

$$\langle(\Delta I)^2\rangle_{\delta\nu} = \frac{4e^2\delta\nu}{\pi\hbar}k_B\Theta T \ , \tag{2.14}$$

which coincides with the result of Ref. 14.

Between these two limits, the noise is a combination of thermal and excess noise. Choosing the energy scales so that the bottom of the conduction band corresponds to $E=0$, we can evaluate the integrals of Eq. (2.11):

$$\int_0^\infty dE\, f_2(1-f_1) = \frac{\mu_1-\mu_2}{2\sinh[(\mu_1-\mu_2)/2k_B\Theta]} \times\exp[-(\mu_1-\mu_2)/2k_B\Theta] \ , \tag{2.15a}$$

$$\int_0^\infty dE(f_1-f_2) = \mu_1-\mu_2 \ , \tag{2.15b}$$

$$\int_0^\infty dE(f_1-f_2) = (\mu_1-\mu_2)\coth[(\mu_1-\mu_2)/2k_B\Theta] - 2k_B\Theta \ . \tag{2.15c}$$

This allows us to give the result for arbitrary temperature:

$$\begin{aligned}\langle(\Delta I)^2\rangle_{\delta\nu} &= \frac{4e^2\delta\nu}{\pi\hbar}k_B\Theta+\frac{2e^2\delta\nu}{\pi\hbar}T(1-T)(\mu_1-\mu_2) \\ &\quad +\frac{4e^2\delta\nu}{\pi\hbar}T(1-T)k_B\Theta \\ &\quad \times\left[\frac{(\mu_1-\mu_2)/k_B\Theta}{\exp[(\mu_1-\mu_2)/k_B\Theta]-1}-1\right] . \end{aligned} \tag{2.16}$$

At high temperatures, the first term on the right-hand side dominates, while the second term leads to the zero-temperature result. The last term in Eq. (2.16) gives the

first-order corrections to the shot-noise and thermal-noise limits. Note that there is no clear separation between these two contributions.

III. MULTICHANNEL CASE

The preceding section dealt with quasi-one-dimensional wires, where only one channel propagates in the ideal leads connected to the sample. For wider leads several transverse states can coexist in the leads at the Fermi level. Our description of electron transport, therefore, has to be generalized to allow several simultaneous wave packets to enter the sample, from a particular incident direction. In this section, we will propose a method for calculating excess noise in a sample connected on the right and on the left to two ideal wide leads, which for the sake of generality will be allowed to carry M channels on the left-hand side and N channels on the right-hand side.

In the conventional description of quantum transport,[26] the sample is described by an $M+N$ by $M+N$ matrix called the S matrix, which determines the amplitudes of the outgoing waves in the leads, given the amplitude of the waves incident on the sample. This definition relies on a choice of basis for the states in the ideal leads, such as the transverse eigenstates of a narrow wire. The transmissive properties are contained in two submatrices of the S matrix, an $N\times M$ matrix $\underline{s}_{21}$ for transmission to the right and an $M\times N$ matrix $\underline{s}_{12}$ for transmission to the left. The reflective properties are specified by the reflection matrices $\underline{s}_{11}$ ($M\times M$ matrix) and $\underline{s}_{22}$ ($N\times N$ matrix). Without loss of generality, one can write the S matrix for a two-terminal sample in the following form:

$$\underline{S}=\begin{bmatrix}\underline{s}_{11} & \underline{s}_{12}\\ \underline{s}_{21} & \underline{s}_{22}\end{bmatrix}. \tag{3.1}$$

To illustrate this formalism, let $\xi_i(x_t)$ denote the wave function associated with transverse channel i in the lead ($i=1,2,\ldots,N$), and let $k_i(E)$ denote the set of longitudinal wave vectors corresponding to each channel, at energy E. The wave function associated with electrons injected from the left-hand side of the sample in a given channel l has the form

$$\psi_{l,E}(x_t,z)=\left[\frac{dk_l}{dE}\right]^{1/2}\xi_l(x_t)e^{ik_l(E)z}+\sum_j \underline{s}_{11}^{jl}\left[\frac{dk_j}{dE}\right]^{1/2}\xi_j(x_t)e^{-ik_j(E)z} \tag{3.2}$$

on the left side of the sample, and

$$\psi_{l,E}(x_t,z)=\sum_j \underline{s}_{21}^{jl}\left[\frac{dk_j}{dE}\right]^{1/2}\xi_j(x_t)e^{ik_j(E)z} \tag{3.3}$$

on the right side of the sample. If we now picture a situation where many incident states are occupied, and we detect what fraction of the incident flux ends up in a given outgoing channel, the S matrix can be used to specify what mixture of these incident states is contained in this outgoing channel [see Fig. 2(a)]. Each channel has a weight factor $(dk_i/dE)^{1/2}$, proportional to the square root of the density of states. For a given energy E, waves in different channels travel at different longitudinal velocities, and the density-of-states factors normalize each channel to a unit flux.

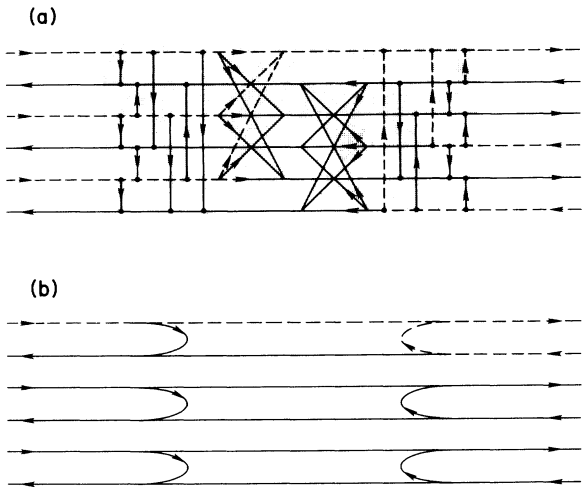

FIG. 2. Invertible case. (a) Schematic representation of mixing between incident and outgoing channels in the sample. The sample is connected on both sides with three propagating channels. Vertical lines represent the transfer from incoming channels to outgoing channels. (b) In the representation of channels specified by the transformation of Eq. (3.6), the sample simply reduces to a set of decoupled one-dimensional channels.

We now turn to the wave-packet construction for the lead with M channels. In principle, we could assign to each wave packet a transverse eigenstate of the leads, so that wave packets that are orthogonal initially, because they are in different channels, remain orthogonal. Following the example of Sec. II [Eq. (2.1)], we can construct a set of orthogonal wave packets that describes the details of electronic transport as follows:

$$\phi_i^{(n)}(x_t,z,t)=\int_{E-\Delta E/2}^{E+\Delta E/2}dE'\frac{1}{\Delta E}\left[\frac{1}{2\pi}\frac{dk_i}{dE'}\right]^{1/2}\xi_i(x_t)\times e^{ik_i(E')z}e^{-iE'(t+n\tau)/\hbar}, \tag{3.4}$$

with i the channel index and n identifying the time slot in which the wave packet is sent. Note that many other constructions of this type can be generated by simply choosing a different basis for the transverse states, or by adding an energy-dependent phase factor in the integrand of Eq. (3.4). As far as the ideal leads are concerned, the generalization of the wave-packet construction to the multichannel case is a trivial one.

A. Diagonal representation, $M=N$

We start with a specific case considered by Lesovik.[15] At zero temperature with a sample connected to the left and right by two identical leads (same number of channels) the transmission matrix for the sample was assumed to be diagonal. As before, we fix the left (right) reservoir

at a chemical potential μ_1 (μ_2), with $\mu_1 > \mu_2$. Wave packets from reservoir 1 in the energy range $[\mu_2,\mu_1]$ can be partially transmitted to the right, with no electrons arriving from reservoir 2. Since the transmission matrix from left to right is diagonal, there is no mixing between channels, and the excess noise is simply a sum of contributions of the type shown in Eq. (2.12). We sum over all channels, with a transmission probability for each channel equal to the square modulus of the corresponding eigenvalue of the transmission matrix. We shall now show that the assumption that the transmission matrix is diagonal is, in fact, unnecessary, and thereby confirm the results of Ref. 17.

In general, an electron incident on the sample can be partially reflected, or partially transmitted through the sample. Unless the transmission and reflection matrices are diagonal, we expect that wave packets from different incident channels will interfere with each other after reaching the sample region. Either we have to take into account these interference effects, or we must find a way around this issue by finding a representation where interdependence between wave packets in the calculation of net transmission is absent.

The scattering probabilities for each incident channel into all the emerging channels must add up to 1. This requires a unitary S matrix, i.e.,

$$\underline{S}^{\dagger}\underline{S}=\underline{S}\,\underline{S}^{\dagger}=\underline{1}\ . \tag{3.5}$$

Let us first examine the case where we have the same number of channels on the two sides of the sample ($N=M$). In Appendix A, we show that if the matrix $\underline{s}_{11}^{\dagger}\underline{s}_{11}$ has no eigenvalues which are equal to 0 or 1, then the following decomposition exists:

$$\begin{aligned}&\underline{s}_{11}=-i\underline{V}_1\underline{R}^{1/2}\underline{U}_1^{\dagger},\quad \underline{s}_{12}=\underline{V}_1\underline{T}^{1/2}\underline{U}_2^{\dagger}\ ,\\ &\underline{s}_{21}=\underline{V}_2\underline{T}^{1/2}\underline{U}_1^{\dagger},\quad \underline{s}_{22}=-i\underline{V}_2\underline{R}^{1/2}\underline{U}_2^{\dagger}\ ,\end{aligned} \tag{3.6}$$

where $\underline{R}^{1/2}$ and $\underline{T}^{1/2}$ are real, diagonal matrices, and $\underline{U}_1$, $\underline{U}_2$, $\underline{V}_1$, and $\underline{V}_2$ are unitary transformations. Such a decomposition has been pointed out in the past,[27] in the context of the transfer matrix. In the present context, this decomposition is the result of a collaboration with Büttiker.[28] The decomposition of Eq. (3.6) is unique, up to a permutation of the eigenvalues of $\underline{R}^{1/2}$ or $\underline{T}^{1/2}$.

At the beginning of this section, we gave an example of wave-packet construction for the multichannel case based on the transverse eigenstates in the ideal leads. This choice of representation is not unique, as any unitary transformation acting on the transverse states can lead to an alternative wave-packet construction. The transformations $\underline{U}_1$, $\underline{U}_2$, $\underline{V}_1$, and $\underline{V}_2$ can be exploited to obtain an additional representation for the states in the leads: $\underline{U}_1$ ($\underline{U}_2$) specifies a unitary transformation for the states *incoming* from the left (right), while $\underline{V}_1$ ($\underline{V}_2$) specifies a unitary transformation for the states *outgoing* to the right (left).

The key ingredient of the decomposition of Eqs. (3.6) is the fact that on a given side of the sample, the *same* unitary transformation describes all the outgoing states, transmitted or reflected. In the new representation, the S matrix takes the form

$$\tilde{\underline{S}}=\begin{pmatrix} -iR_1^{1/2} & \cdots & 0 & T_1^{1/2} & \cdots & 0 \\ \vdots & \ddots & \vdots & \vdots & \ddots & \vdots \\ 0 & \cdots & -iR_M^{1/2} & 0 & \cdots & T_M^{1/2} \\ T_1^{1/2} & \cdots & 0 & -iR_1^{1/2} & \cdots & 0 \\ \vdots & \ddots & \vdots & \vdots & \ddots & \vdots \\ 0 & \cdots & T_M^{1/2} & 0 & \cdots & -iR_M^{1/2} \end{pmatrix}. \tag{3.7}$$

i.e., the nonzero elements are only on the diagonal of the four submatrices. In this representation, the sample can be thought of as a set of single-channel samples which are decoupled from each other [see Fig. 2(b)].

In the diagonal representation, the wave packets incident from the left-hand side will now have the form

$$\phi_j^{(n)}(x_t,z,t)=\int_{E-\Delta E/2}^{E+\Delta E/2}dE'\frac{1}{\Delta E}\sum_{i=1}^{N}U_1^{ij}(E')\left[\frac{1}{2\pi}\frac{dk_i}{dE'}\right]^{1/2}\xi_i(x_t)e^{ik_i(E')z}e^{-iE'(t+n\tau)/\hbar}\ . \tag{3.8}$$

A similar construction exists for the wave packets incident from the right-hand side, with the unitary transformation U_2. Synchronism between wave packets coming from opposite sides of the sample is necessary only to the extent that wave packets belong to the same one-dimensional eigenchannel.

The absence of correlations between these wave packets permits us to write down the general result for the excess noise in a multichannel two-terminal structure as a sum over eigenvalues, each eigenvalue giving a contribution of the form Eq. (2.11):

$$\begin{aligned}\langle(\Delta I)^2\rangle=&\frac{4e^2\delta\nu}{\pi\hbar}\int dE\sum_{i=1}^{N}T_i(E)f_2(1-f_1)\\ &+\frac{2e^2\delta\nu}{\pi\hbar}\int dE\sum_{i=1}^{N}T_i(E)(f_1-f_2)\\ &\times[1-T_i(E)(f_1-f_2)]\ .\end{aligned} \tag{3.9}$$

As anticipated in the beginning of this section, this result has precisely the form of that of Lesovik,[15] who assumed

from the start that the S matrix has the structure of Eq. (3.7). In the general case, the decomposition of the S matrix outlined in this section leads us to a representation through channels that do *not* interfere, which brings us back to the simplicity of the uncoupled channels assumed by Lesovik. The reader must be cautioned: the apparent simplicity of Eq. (3.9) is not readily accessible to the experimentalist. Our noninterfering channels were constructed from knowledge of the S matrix; and only in the simplest of situations will this be known for a real sample. If the S matrix is determined by the geometry of the sample, as determined by lithography, then we may be able to calculate an S matrix. If the S matrix is determined by the location of randomly placed point scatterers, it will not be easily ascertained.

B. Noninvertible and nonsymmetric case, $M \neq N$

We will now show how Eq. (3.9) can be generalized to arbitrary situations, where a decomposition of the type (3.6) does not exist.

We start with the noninvertible case, for $M = N$. The matrix $\underline{s}_{11}^{\dagger}\underline{s}_{11}$ then has eigenvalues that are equal to 0 or 1. In Appendix A, we point out that a decomposition of the type Eqs. (3.6) still exists, but only for the eigenvalues of this matrix that differ from both 0 or 1. These remaining eigenvalues have to be treated separately. In the remainder of this paper, we use the word *eigenchannels* for the set of channels constructed from the eigenstates of the transmission and reflection matrices. An eigenvalue 0 corresponds to an incident eigenchannel that is perfectly transmitted: the reflection coefficient for waves incident on both sides of the sample is zero, so that the transmitted wave is not related to a reflected eigenchannel as in the invertible case. This eigenchannel therefore can only give a contribution to thermal equilibrium noise, which corresponds to the first term on the right-hand side of Eq. (3.9). An eigenvalue 1 corresponds to an eigenchannel that is totally reflected and therefore is not coupled to other eigenchannels on the other side of the sample. Since $T_i = 0$, this eigenvalue does not give any contribution to Eq. (3.9). This is illustrated in Fig. 3(a): eigenvalues that describe partial reflection/transmission require that the corresponding outgoing eigenchannels collect states incident from both sides of the sample. No such restriction exists for total reflection/transmission.

The nonsymmetric case ($M \neq N$) can be understood in a similar manner. For $M > N$, the S matrix can be extended to an $2M \times 2M$ matrix, by adding rows and columns to the matrices $\underline{s}_{22}$, $\underline{s}_{12}$, and $\underline{s}_{21}$ in such a way that the new S matrix keeps its unitarity: it simply amounts to adding a set of $M - N$ passive channels that are totally reflected on the side with only N channels. From this new S matrix, we can then repeat the argument of the preceding paragraph to obtain the expression for combined thermal and excess noise: channels that are totally reflected do not give any contribution in Eq. (3.9).

Before ending this section, we can ask whether this type of diagonal decomposition is not too far removed from what happens in the laboratory. We know at least one example where electrons behave exactly as described above: electrons confined to a two-dimensional plane in a high perpendicular magnetic field.[29] A bias is applied between the two sides of the sample, allowing current flow. In the direction perpendicular to the current, a confinement potential can be achieved by means of electrostatic gates, allowing only a few sets of channels to propagate through the sample.[30] In the presence of a strong magnetic field, electrons travel from one side of the sample to the other along so-called edge states,[31,32] which are the quantum analog of the classical skipping orbits. If a metallic gate is placed in the middle of the sample, electrons from the innermost edge states can be backscattered, as illustrated in Fig. 3(b). Incidentally, Fig. 3(b) describes the geometry of the noise experiment of Ref. 13, initially suggested by Büttiker.[17] Although Fig. 3(b) gives a simplified view that ignores scattering between edge states, in this particular case the S matrix associated with this situation has precisely the structure of Eq. (3.7).

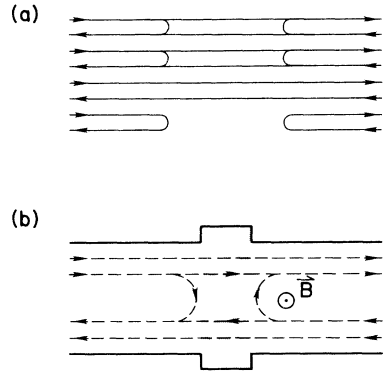

FIG. 3. (a) Noninvertible case: if the transmission-reflection matrices have zero eigenvalues, the sample can still be regarded as a set of decoupled channels. Channel 3 is perfectly transmitted, and channel 4 is totally reflected; it does not couple to the other side of the sample. (b) Transport of electrons confined to two dimensions in a perpendicular magnetic field. The dotted line represents the edge states, and the shaded region represents a metallic gate which causes the electrons to backscatter. Note the analogy with (a).

IV. MULTITERMINAL CASE

Until now, we have limited the discussion to two-terminal samples. The situation where the sample is actually connected to many leads is of practical interest; an example is the Hall bar geometry. Büttiker[32] proposed a scattering matrix approach for the quantum Hall effect, treating current supply and voltage probe contacts on an equal footing. From the reflection and transmission properties of the multiterminal sample, Büttiker was able to predict the quantization of the Hall conductance. Here, we will extend the reservoir picture to calculate the noise in current at *zero temperature* with our wave-packet method.

A. Current noise in an arbitrary lead

The sample is connected to the reservoirs by ideal leads, as in the two-terminal case. To each reservoir γ

($\gamma=1,2,\ldots,P$), we attribute a chemical potential μ_γ. The reservoirs are numbered in order of decreasing chemical potential:

$$\mu_1>\mu_2>\cdots>\mu_\gamma>\cdots>\mu_P \ .$$

This situation is illustrated in Fig. 4. For simplicity, we assume that each lead connected to the sample carries the same number of channels, N. To calculate the noise, we consider separately the contribution coming from each energy range $[\mu_{\gamma+1},\mu_\gamma]$. Current flow in this structure can be understood in terms of electron transport from one lead to another, or alternatively in terms of hole transport in the opposite direction. In the above energy range, electrons (holes) travel from leads $\gamma'\leq\gamma$ ($\gamma'>\gamma$) to leads $\gamma'>\gamma$ ($\gamma'\leq\gamma$). This very separation between *injecting* leads and *receiving* leads suggests that the tools developed in the preceding section for the two-terminal sample can be used here.

We make a distinction between the contribution from energy ranges above and below μ_α, the chemical potential of the reservoir connected to the sample through lead α where we shall calculate the noise.

For energies above μ_α, lead α belongs to the group of leads that receives electrons. Consider the contribution from the energy range $[\mu_{\gamma+1},\mu_\gamma]$. We have a situation similar to the two-terminal case with a different number of channels on each side of the sample: leads 1 to γ can be pictured as one single lead with $\gamma\times N$ channels that injects electrons in α. Transmission into lead α is thus characterized by an N by $\gamma\times N$ transmission matrix of the form

$$\underline{t}_{\gamma\alpha}=(\underline{s}_{\alpha 1}\ \ \underline{s}_{\alpha 2}\ \ \cdots\ \ \underline{s}_{\alpha\gamma}) \ , \tag{4.1}$$

where the first index specifies how many injecting leads are involved, and the second index identifies the lead where noise is measured. This matrix is all we need to calculate the noise in lead α at zero temperature. The transmission probabilities that enter in Eq. (3.9) now replaced by the eigenvalues of the matrix

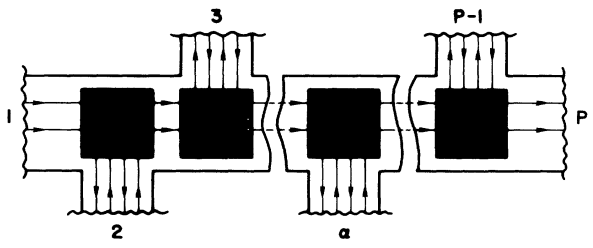

FIG. 4. Multiterminal sample: each lead carries two channels, and the arrows specify the direction of electron motion, as constrained by Fermi blocking at zero temperature. The shaded boxes represent the mixing between channels (the fact that the spatial sequence of the reservoirs agrees with the ordering of the chemical potentials is only for simplicity, and not part of the argument).

$$\underline{t}^\dagger_{\gamma\alpha}\underline{t}_{\gamma\alpha}=\begin{pmatrix} s^\dagger_{\alpha 1}s_{\alpha 1} & s^\dagger_{\alpha 1}s_{\alpha 2} & \cdots & s^\dagger_{\alpha 1}s_{\alpha\gamma} \\ s^\dagger_{\alpha 2}s_{\alpha 1} & s^\dagger_{\alpha 2}s_{\alpha 2} & \cdots & s^\dagger_{\alpha 2}s_{\alpha\gamma} \\ \vdots & \vdots & \ddots & \vdots \\ s^\dagger_{\alpha\gamma}s_{\alpha 1} & s^\dagger_{\alpha\gamma}s_{\alpha 2} & \cdots & s^\dagger_{\alpha\gamma}s_{\alpha\gamma} \end{pmatrix} . \tag{4.2}$$

Let $T_i^{\gamma\alpha}$ ($i=1,2,\ldots,\gamma N$) denote these eigenvalues. In general, each of the corresponding eigenvectors of the matrix $\underline{t}^\dagger_{\gamma\alpha}\underline{t}_{\gamma\alpha}$ is a superposition of channel states from *different* injecting leads. Now, wave packets emerging from one reservoir, via a lead, are incoherent with those coming out of another reservoir, into its lead. Our use of incoming wave packets that are coherent over a number of leads is probably an unnecessary complication, avoidable in an alternative formulation which does not yet exist, except in the very limited way discussed in Sec. VI. Such an alternative formulation will, presumably, yield identical results but demonstrate more explicitly the fact that these results do not really depend on coherence between different leads. Consider the density matrix ρ characteristizing the wave packets emerging from the reservoirs into the leads. ρ is diagonal in a representation in which the wave packets occupy very narrow energy ranges, and assigns an occupation probability to each packet corresponding to the Fermi occupation probability. We have used a representation in which the wave packets invoke coherent behavior between different leads. But, of course, we could with equal justification use wave packets coming from a single lead, characterized by the same density matrix and occupation probability. In that case, however, the subsequent noise evaluation is less straightforward, but must nevertheless lead to our result.

Summing up over contributions of the type Eq. (2.12) for each eigenvalue, the noise-power spectrum coming from the energy range $[\mu_{\gamma+1},\mu_\gamma]$ with $\alpha>\gamma$ reduces to

$$\langle(\Delta I_\alpha)^2\rangle_{\delta\nu,[\mu_{\gamma+1},\mu_\gamma]}=\frac{2e^2\delta\nu}{\pi\hbar}(\mu_\gamma-\mu_{\gamma+1}) \times\sum_{i=1}^{\gamma N}T_i^{\gamma\alpha}(1-T_i^{\gamma\alpha}) \ . \tag{4.3}$$

To establish a connection between this result and that of Ref. 17, we can express this last result in terms of the coefficients of the S matrix. In Appendix B, we show that the sum over eigenvalues in Eq. (4.3) can be written as a trace of the matrix

$$\mathrm{Tr}[\underline{t}^\dagger_{\gamma\alpha}\underline{t}_{\gamma\alpha}(\underline{1}-\underline{t}^\dagger_{\gamma,\alpha}\underline{t}_{\gamma,\alpha})]=\sum_{\eta\leq\gamma<\delta}\mathrm{Tr}(\underline{s}_{\alpha\delta}\underline{s}^\dagger_{\alpha\delta}\underline{s}_{\alpha\eta}\underline{s}^\dagger_{\alpha\eta}) \ . \tag{4.4}$$

The unitarity of the S matrix was used to derive the preceding expression.

Next, we turn to energy ranges below μ_α. Here, lead α injects electrons into leads $\gamma+1,\gamma+2,\ldots,P$ ($\alpha\leq\gamma$). Alternatively, we can think of holes being injected into lead α from these leads. The transport properties of holes are then described by an N by $(P-\gamma)\times N$ transmission matrix:

$$\tilde{\underline{t}}_{\gamma\alpha}=(\underline{s}_{\alpha,\gamma+1}\ \underline{s}_{\alpha,\gamma+2}\ \cdots\ \underline{s}_{\alpha P})\ , \tag{4.5}$$

and the transmission probabilities are now the eigenvalues $\tilde{T}_i^{\gamma\alpha}$ ($i=\gamma\times N+1,\ldots,P\times N$) of the matrix $\tilde{\underline{t}}^{\dagger}_{\gamma\alpha}\tilde{\underline{t}}_{\gamma\alpha}$. The contribution from the energy range $[\mu_{\gamma+1},\mu_\gamma]$ for $\gamma<\alpha$ thus reduces to

$$\langle(\Delta I_\alpha)^2\rangle_{\delta\nu,[\mu_{\gamma+1},\mu\gamma]}=\frac{2e^2\,\delta\nu}{\pi\hbar}(\mu_\gamma-\mu_{\gamma+1})\times\sum_{i=\gamma N+1}^{PN}\tilde{T}_i^{\gamma\alpha}(1-\tilde{T}_i^{\gamma\alpha})\ . \tag{4.6}$$

Again, this sum can be expressed as a trace (see Appendix B):

$$\mathrm{Tr}[\tilde{\underline{t}}^{\dagger}_{\gamma,\alpha}\tilde{\underline{t}}_{\gamma\alpha}(\underline{1}-\tilde{\underline{t}}^{\dagger}_{\gamma,\alpha}\tilde{\underline{t}}_{\gamma\alpha})]=\sum_{\eta\le\gamma<\delta}\mathrm{Tr}(\underline{s}_{\alpha\delta}\underline{s}^{\dagger}_{\alpha\delta}\underline{s}_{\alpha\eta}\underline{s}^{\dagger}_{\alpha\eta})\ , \tag{4.7}$$

which is of similar form as Eq. (4.4).

We now sum up the contribution of all energy intervals, for energy ranges above and below μ_α:

$$\langle(\Delta I_\alpha)^2\rangle_{\delta\nu}=\frac{2e^2\,\delta\nu}{\pi\hbar}\sum_{\eta<\delta}(\mu_\delta-\mu_\eta)\,\mathrm{Tr}(\underline{s}_{\alpha\delta}\underline{s}^{\dagger}_{\alpha\delta}\underline{s}_{\alpha\eta}\underline{s}^{\dagger}_{\alpha\eta})\ ,$$

which is precisely the result of Ref. 17.

B. Noise correlations

Our wave-packet approach can be extended to the calculation of noise correlation between different leads. To illustrate this, we consider the simple case where the leads α and β for which correlation is measured have the same chemical potential ($\mu_\alpha=\mu_\beta$). Grouping leads α and β into one single lead ($\alpha+\beta$), we calculate the noise in this new lead.

Above μ_α, electrons in an energy range $[\mu_{\gamma+1},\mu_\gamma]$ are injected into $(\alpha+\beta)$ from leads $1,2,\ldots,\gamma$. The transmission matrix that describes this process is

$$\underline{t}_{\gamma(\alpha+\beta)}=\begin{pmatrix}\underline{s}_{\alpha1} & \underline{s}_{\alpha2} & \cdots & \underline{s}_{\alpha\gamma}\\ \underline{s}_{\beta1} & \underline{s}_{\beta2} & \cdots & \underline{s}_{\beta\gamma}\end{pmatrix}\ . \tag{4.8}$$

Following the prescription of the preceding subsection for calculation of noise in this energy range, the eigenvalues $T_i^{\gamma(\alpha+\beta)}$ ($i=1,2,\ldots,\gamma N$) of the matrix $\underline{t}^{\dagger}_{\gamma(\alpha+\beta)}\underline{t}_{\gamma(\alpha+\beta)}$ specify the transmission properties of each eigenchannel, giving a noise contribution

$$\langle(\Delta I_{(\alpha+\beta)})^2\rangle_{\delta\nu,[\mu_{\gamma+1},\mu_\gamma]}=\frac{2e^2\,\delta\nu}{\pi\hbar}(\mu_\gamma-\mu_{\gamma+1})\sum_{i=1}^{\gamma N}T_i^{\gamma(\alpha+\beta)}(1-T_i^{\gamma(\alpha+\beta)})\ . \tag{4.9}$$

Below μ_α we consider the transfer of holes into lead $(\alpha+\beta)$ with the matrix

$$\tilde{\underline{t}}_{\gamma(\alpha+\beta)}=\begin{pmatrix}\underline{s}_{\alpha,\gamma+1} & \underline{s}_{\alpha,\gamma+2} & \cdots & \underline{s}_{\alpha P}\\ \underline{s}_{\beta,\gamma+1} & \underline{s}_{\beta,\gamma+2} & \cdots & \underline{s}_{\beta P}\end{pmatrix}\ . \tag{4.10}$$

This leads to a contribution

$$\langle(\Delta I_{(\alpha+\beta)})^2\rangle_{\delta\nu,[\mu_{\gamma+1},\mu_\gamma]}=\frac{2e^2\,\delta\nu}{\pi\hbar}(\mu_\gamma-\mu_{\gamma+1})\sum_{i=1}^{\gamma N}\tilde{T}_i^{\gamma(\alpha+\beta)}(1-\tilde{T}_i^{\gamma(\alpha+\beta)})\ , \tag{4.11}$$

with $\tilde{T}_i^{\gamma(\alpha+\beta)}$ ($i=\gamma N+1,\ldots,PN$), representing the eigenvalues of the matrix $\tilde{\underline{t}}_{\gamma(\alpha+\beta)}\tilde{\underline{t}}_{\gamma(\alpha+\beta)}$. In Appendix B, we rewrite the two sums over eigenvalues in Eqs. (4.9) and (4.11) in terms of the block elements of the S matrix.

Regrouping the contribution of energy ranges above and below μ_α, we determine the excess noise in lead $\alpha+\beta$ to be

$$\langle(\Delta I_{(\alpha+\beta)})^2\rangle_{\delta\nu}=\langle(\Delta I_\alpha)^2\rangle_{\delta\nu}+\langle(\Delta I_\beta)^2\rangle_{\delta\nu}-\frac{4e^2\,\delta\nu}{\pi\hbar}\sum_{\eta>\delta}(\mu_\delta-\mu_\eta)\times\mathrm{Tr}(\underline{s}_{\alpha\eta}\underline{s}^{\dagger}_{\beta\eta}\underline{s}_{\beta\delta}\underline{s}^{\dagger}_{\alpha\delta})\ . \tag{4.12}$$

The noise current in lead $\alpha+\beta$ can thus be decomposed into three distinct contributions: the noise current in α, the noise current in β, plus an interference term that represents the correlations between α and β, $2\langle\Delta I_\alpha\,\Delta I_\beta\rangle_{\delta\nu}$. As pointed out by Büttiker,[17] for a sample with more than three leads, the correlations between two leads cannot be expressed in terms of probabilities (elements of the S matrix multiplied by their complex conjugates). Büttiker suggests that this permits the observation of interference effects in the measurement of correlations, even if the interfering paths originate in different reservoirs that emit incoherently.

At this point, we have not managed to generalize our multichannel results to finite temperatures. Reference 17 does not suffer from this limitation, as in this case Fermi factors are the result of averages of products of creation and annihilation operators.

V. NOISE CORRELATIONS IN A Y-SHAPED STRUCTURE

We illustrate the formalism developed in the preceding sections with a simple example: the calculation of noise correlations between two leads which divide the electrons emitted from a third lead. A long time ago, an analogous experiment for photons was performed by Hanbury Brown and Twiss,[33] measuring the correlations between two photomultipliers detecting light from a coherent source. The resulting observation of a positive correlation between the two detectors was correctly attributed to the fact that photons are undistinguishable particles which obey Bose-Einstein statistics.[34] It is thus reasonable to ask whether a corresponding effect exists for particles obeying Fermi-Dirac statistics, a question posed by Murphy.[35] Here, we go one step further, applying these ideas to electron transport in multiterminal structures.

Consider the structures described in Fig. 5, with chemical potentials μ_1, μ_2, and μ_3 associated with leads 1, 2, and 3 satisfying the inequality $\mu_1>\mu_2>\mu_3$. Let N be the

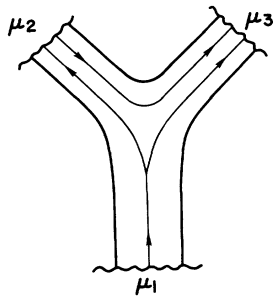

FIG. 5. Y-shaped sample, with $\mu_1>\mu_2>\mu_3$. Lead 1 injects electrons into 2 and 3, where anticorrelated current fluctuations are predicted.

number of channels in each of these leads (as mentioned in Sec. III, we always reduce a system with an arbitrary number of channels in each lead to the present case by a redefinition of the S matrix). At zero temperature, electrons injected from lead 1 can be transmitted into 2 and 3, and lead 2 itself can inject electrons in lead 3.

Before facing the analytical details in their general form, let us consider a somewhat idealized illustrative possibility, closely related to the above-mentioned suggestion by Murphy. Let $\mu_2=\mu_3$, let all the leads be single-channel leads, and let us specialize to the low-temperature limit. Assume that the Y of Fig. 5, near its junction, consists of a slowly and smoothly varying potential, symmetrical about the vertical axis. Assume that the injecting lead widens adiabatically to twice its original width, as it approaches the junction. Then all the carriers coming up along lead 1 will be transmitted with equal probability into leads 2 and 3, and without reflection back into lead 1. All the states or wave packets in lead 1, between μ_2 and μ_1, will be filled. The stream in lead 1 is noiseless. Leads 2 and 3 will each have their wave packets half occupied, resulting in noise according to Eq. (2.12). The sum of these noise currents, however, must vanish. Thus the two leads have perfectly anticorrelated noise. When more electrons, in a given time interval, enter lead 2, fewer will enter lead 3.

Related effects were discussed in the vacuum tube literature.[22] As we have mentioned, Coulomb interaction can produce "space-charge smoothing," regulating the flow of electrons, and thus reducing noise below the shot-effect value predicted from the current flow actually present. If a part of the regulated beam is then intercepted, we destroy the regularity of the remaining beam produced by Coulomb interaction, and push the noise in this remaining portion closer toward its shot-noise value. In our case, the regularity in the original undivided beam is not a result of Coulomb effects, but of the Pauli principle. But as in the case of vacuum tube, partition noise, randomly selecting a part of the incident beam, reduces the correlation and increases the relative noise.

Now let us return to the more general treatment. To calculate the correlations between 2 and 3, we proceed as before:

$$\langle \Delta I_2\,\Delta I_3\rangle_{\delta\nu}=\tfrac{1}{2}[\langle(\Delta I_{(2+3)})^2\rangle_{\delta\nu}-\langle(\Delta I_2)^2\rangle_{\delta\nu}-\langle(\Delta I_3)^2\rangle_{\delta\nu}]\ . \tag{5.1}$$

We thus have to evaluate the noise terms on the right-hand side of this equation for the two energy ranges $[\mu_2,\mu_1]$ and $[\mu_3,\mu_2]$.

In the energy range $[\mu_2,\mu_1]$, electrons are injected from lead 1. For transmission into lead 2, we then have

$$\langle(\Delta I_2)^2\rangle_{\delta\nu[\mu_2,\mu_1]}=\frac{2e^2\delta\nu}{\pi\hbar}(\mu_1-\mu_2)\times\mathrm{Tr}[\underline{s}_{21}^{\dagger}\underline{s}_{21}(1-\underline{s}_{21}^{\dagger}\underline{s}_{21})]\ , \tag{5.2}$$

and similarly for lead 3,

$$\langle(\Delta I_3)^2\rangle_{\delta\nu[\mu_2,\mu_1]}=\frac{2e^2\delta\nu}{\pi\hbar}(\mu_1-\mu_2)\times\mathrm{Tr}[\underline{s}_{31}^{\dagger}\underline{s}_{31}(1-\underline{s}_{31}^{\dagger}\underline{s}_{31})]\ . \tag{5.3}$$

In a lead constituted by grouping 2 and 3, the transmission matrix has the form of Eq. (4.8), and we obtain

$$\langle(\Delta I_{(2+3)})^2\rangle_{\delta\nu[\mu_2,\mu_1]}=\langle(\Delta I_2)^2\rangle_{\delta\nu[\mu_2,\mu_1]}+\langle(\Delta I_3)^2\rangle_{\delta\nu[\mu_2,\mu_1]}-\frac{4e^2\delta\nu}{\pi\hbar}(\mu_1-\mu_2)\times\mathrm{Tr}(\underline{s}_{21}^{\dagger}\underline{s}_{21}\underline{s}_{31}^{\dagger}\underline{s}_{31})\ . \tag{5.4}$$

In the energy range $[\mu_3,\mu_2]$, electrons flow from 1 and 2 into 3. Alternatively, holes are injected from 3 into 1 and 2. This leads to the result

$$\langle(\Delta I_2)^2\rangle_{\delta\nu[\mu_3,\mu_2]}=\frac{2e^2\delta\nu}{\pi\hbar}(\mu_2-\mu_3)\times\mathrm{Tr}[\underline{s}_{23}^{\dagger}\underline{s}_{23}(1-\underline{s}_{23}^{\dagger}\underline{s}_{23})]\ . \tag{5.5}$$

For the noise in lead 3, we use Eqs. (4.3) and (4.4):

$$\langle(\Delta I_3)^2\rangle_{\delta\nu[\mu_3,\mu_2]}=\frac{2e^2\delta\nu}{\pi\hbar}(\mu_2-\mu_3)\times\mathrm{Tr}[\underline{s}_{33}\underline{s}_{33}^{\dagger}(\underline{s}_{31}\underline{s}_{31}^{\dagger}+\underline{s}_{32}\underline{s}_{32}^{\dagger})]\ . \tag{5.6}$$

In this energy range, the noise in lead (2+3) comes from holes transmitted from 3 into 1 only, which gives

$$\langle(\Delta I_{(2+3)})^2\rangle_{\delta\nu[\mu_3,\mu_2]}=\frac{2e^2\delta\nu}{\pi\hbar}(\mu_2-\mu_3)\times\mathrm{Tr}[\underline{s}_{13}^{\dagger}\underline{s}_{13}(1-\underline{s}_{13}^{\dagger}\underline{s}_{13})]\ . \tag{5.7}$$

Summing up the contribution from the two energy ranges considered and using Eq. (5.1), we get an expression for the correlations:

$$\langle\Delta I_2\,\Delta I_3\rangle_{\delta\nu}=-\frac{2e^2\delta\nu}{\pi\hbar}[(\mu_1-\mu_2)\,\mathrm{Tr}(\underline{s}_{21}^{\dagger}\underline{s}_{21}\underline{s}_{31}^{\dagger}\underline{s}_{31})+(\mu_2-\mu_3)\,\mathrm{Tr}(\underline{s}_{23}^{\dagger}\underline{s}_{23}\underline{s}_{33}^{\dagger}\underline{s}_{33})]\ . \tag{5.8}$$

Note that the correlations are always negative: using the cyclic property of the trace, both traces on the right-hand side of Eq. (5.8) can be written as the trace of a Hermitian matrix, and the trace of a Hermitian matrix is always positive. The current fluctuations between these two

leads are *anticorrelated*. This is a direct consequence of the fact that electrons obey Fermi statistics. This result has been noted by Büttiker,[36] who also showed that if electrons are replaced by bosons, the resulting correlations become positive, in agreement with the Hanbury Brown and Twiss experiment.

In principle, this effect should be observable experimentally. If we assume that the two receiving leads have the same chemical potential, Eq. (5.8) further simplifies, and we can normalize the noise correlations as follows:

$$\frac{\langle \Delta I_2 \Delta I_3 \rangle_{\delta\nu}}{\langle (\Delta I_2)^2 \rangle_{\delta\nu}^{1/2} \langle (\Delta I_3)^2 \rangle_{\delta\nu}^{1/2}} = \frac{-\mathrm{Tr}(\underline{s}_{31}^{\dagger}\underline{s}_{31}\underline{s}_{21}^{\dagger}\underline{s}_{21})}{\{\mathrm{Tr}[\underline{s}_{31}^{\dagger}\underline{s}_{31}(1-\underline{s}_{31}^{\dagger}\underline{s}_{31})]\,\mathrm{Tr}[\underline{s}_{21}^{\dagger}\underline{s}_{21}(1-\underline{s}_{21}^{\dagger}\underline{s}_{21})]\}^{1/2}} . \tag{5.9}$$

In the simplest case, where one channel can propagate in each lead, the traces drop out of this equation, and the effect is optimized if we arrange the sample so that the electrons from the injecting contact pass on out with little probability of reflection back into that injecting lead.

VI. COHERENCE BETWEEN LEADS

Our results in Sec. IV for the multilead case invoked wave packets that have coherent contributions emerging from different reservoirs. We know, however, that electrons entering a reservoir suffer inelastic scattering before reemerging. They are incoherent, when again emitted, with the stream coming out of other reservoirs. Similarly, in Eq. (3.8) we utilized "eigenchannel" wave packets that have coherent contributions from different channels, with these channels corresponding to the eigenvalues of the original transverse Hamiltonian. But we also know that electrons emerging from a given reservoir, in different channels, can be considered incoherent. As already suggested in Sec. IV, this results in expressions that imply more coherence than they really involve. We will clarify this through an example.

Consider an energy range $[\mu_\gamma,\mu_{\gamma+1}]$ as in Sec. IV, in which reservoirs $1,2,\ldots,\gamma$ are emitting a fully occupied stream of electrons, some of which are transmitted into reservoir α, with $\alpha>\gamma$. Reservoir α and the remaining reservoirs are not emitting in this energy range. For simplicity, we assume that only one channel can propagate in each lead.

Reference 21 analyzed this situation. Let $T_{\alpha 1},\ldots,T_{\alpha\gamma}$ denote the respective *probabilities* of an electron coming out of reservoirs $1,2,\ldots,\gamma$ and ending up in the reservoir connected to lead α. The discussion in Ref. 21 gave an expression for the noise in lead α:

$$\langle (\Delta I_\alpha)^2 \rangle_{\Delta\nu} = \frac{2e^2}{\pi\hbar}(\mu_\gamma-\mu_{\gamma+1}) \left[1-\sum_{\delta=1}^{\gamma} T_{\alpha\delta} \right] \sum_{\delta=1}^{\gamma} T_{\alpha\delta} . \tag{6.1}$$

We stress that the derivation of Eq. (6.1) explicitly invoked a lack of coherence between reservoirs.

Consider now the alternative approach of Sec. IV, which treats the combination of the incoming leads $1,2,\ldots,\gamma$ as one source with γ channels. We then use the "eigenchannels," i.e., the input modes in the combined γ channel lead, whose probability of transmission into lead α can be calculated independently, without attention to interference between the eigenchannels. There can be only one of these eigenchannels with a nonvanishing transmission probability $\tilde{T}_\alpha$ into lead α (if there were two eigenchannels with nonvanishing transmission, then we could get interference between these two). Let us identify the γ eigenchannel incident wave packets by $\tilde{\psi}_1,\ldots,\tilde{\psi}_\gamma$, where $\tilde{\psi}_1$ is associated with the nonvanishing transmission probability $\tilde{T}_\alpha$ into lead α. Let

$$\tilde{\psi}_1 = \sum_{\delta=1}^{\gamma} U_{1\delta}\psi_\delta , \tag{6.2}$$

where $\psi_1,\ldots,\psi_\gamma$ are the normalized wave packets limited to each lead, and the matrix $U_{\beta,\delta}$ defines the unitary transformation for the eigenchannel representation.

We can now proceed to express $T_{\alpha 1},\ldots,T_{\alpha\gamma}$ in terms of $\tilde{T}_\alpha$. For a given emitting lead β, ψ_β can be specified as a sum of eigenchannel wave packets,

$$\psi_\beta = \sum_{\delta=1}^{\gamma} U_{\delta\beta}^{*}\tilde{\psi}_\delta . \tag{6.3}$$

Since only $\tilde{\psi}_1$ contributes to transmission into α, $T_{\alpha\beta}=|U_{1\beta}|^2\tilde{T}_\alpha$. As a result, the sum of the transmission probabilities appearing in Eq. (6.1) becomes

$$\sum_{\delta=1}^{\gamma} T_{\alpha\delta} = \tilde{T}_\alpha \sum_{\delta=1}^{\gamma} |U_{1\delta}|^2 = \tilde{T}_\alpha . \tag{6.4}$$

Therefore, Eq. (6.1) becomes

$$\langle (\Delta I_\alpha)^2 \rangle_{\Delta\nu} = \frac{2e^2}{\pi\hbar}(\mu_\gamma-\mu_{\gamma+1})\tilde{T}_\alpha(1-\tilde{T}_\alpha) , \tag{6.5}$$

in agreement with our treatment in Sec. IV. The apparent dependence, in Eq. (6.5), on the coherent behavior of particular eigenchannels is deceptive.

VII. SUMMARY

We have proposed a wave-packet approach for noise-current calculations in multichannel, multiterminal structures. A description of electron transport was introduced, which takes into account the constraints imposed by the Fermi statistics of the charge carriers in the leads connected to the sample. From this description, we showed that the noise current at low frequencies can be related to the statistics of charge carriers crossing the sample. In one dimension, we noted that excess noise is suppressed both in the case of weak and ideal transmission: in a quantum coherent sample, excess noise can therefore never reach the level of classical shot noise. Turning to the multichannel case, we showed that the calculation of noise can be reduced to a superposition of one-dimensional contributions using an appropriate rep-

resentation for the different transverse channels in the leads connected to the sample. This picture was extended to multiterminal structures at zero temperatures. The principal ingredient of our method lies in the choice of a representation such that the total transmission is the sum of separate transmission probabilities, without cross terms. Finally, we suggested an experiment for electrons injected into one branch of a Y-shaped sample, where current fluctuations in the two receiving leads are anticorrelated.

While it may seem that the wave-packet approach is a naive picture of electron transport, we were able to reproduce the results derived from other more formal approaches with minimal complexity. We believe that this approach captures the essential physics of noise in mesoscopic systems as derived from quantum-mechanical transmission.

ACKNOWLEDGMENT

We have had many fruitful discussions with M. Büttiker, and are particularly indebted to him for his input leading to the decomposition of Appendix A.

APPENDIX A

In this appendix, we derive the diagonal decomposition[27,28] of the reflection and transmission submatrices of Sec. III. We will assume that the number of channels is the same on each side of the sample. If this is not the case, the present decomposition can still be achieved if we add rows and columns to the S matrix so that each subblock $\underline{s}_{11}$, $\underline{s}_{12}$, $\underline{s}_{12}$, and $\underline{s}_{22}$ is a square matrix, as explained in Sec. III B.

From Eq. (3.1), the unitarity property of the S matrix translates into six independent equations:

$$\underline{s}_{11}^{\dagger}\underline{s}_{11}+\underline{s}_{21}^{\dagger}\underline{s}_{21}=\underline{1} , \tag{A1a}$$

$$\underline{s}_{11}\underline{s}_{11}^{\dagger}+\underline{s}_{12}\underline{s}_{12}^{\dagger}=\underline{1} , \tag{A1b}$$

$$\underline{s}_{22}^{\dagger}\underline{s}_{22}+\underline{s}_{12}^{\dagger}\underline{s}_{12}=\underline{1} , \tag{A1c}$$

$$\underline{s}_{22}\underline{s}_{22}^{\dagger}+\underline{s}_{21}\underline{s}_{21}^{\dagger}=\underline{1} , \tag{A1d}$$

$$\underline{s}_{22}\underline{s}_{21}^{\dagger}+\underline{s}_{12}\underline{s}_{22}^{\dagger}=\underline{0} , \tag{A1e}$$

$$\underline{s}_{12}^{\dagger}\underline{s}_{11}+\underline{s}_{22}^{\dagger}\underline{s}_{21}=\underline{0} . \tag{A1f}$$

Without loss of generality, we start by introducing the following decomposition for the matrix $\underline{s}_{11}$:

$$\underline{s}_{11}=\underline{V}_1\underline{D}_{11}\underline{U}_1^{\dagger} , \tag{A2}$$

with unitary matrices $\underline{V}_1$ and $\underline{U}_1$, and $\underline{D}_{11}$ a diagonal matrix. The eigenvalues of the matrices $\underline{s}_{11}^{\dagger}\underline{s}_{11}$ and $\underline{s}_{11}\underline{s}_{11}^{\dagger}$ are then simply the diagonal elements of the matrix $\underline{D}_{11}^{*}\underline{D}_{11}$, where $*$ denotes the complex conjugate. We now proceed to a similar decomposition for the other blocks of the S matrix, taking into account the constraints imposed by Eqs. (A1a)–(A1f).

In a first step, we obtain the decompositions:

$$\begin{aligned}\underline{s}_{21}&=\underline{W}_2\underline{D}_{21}\underline{U}_1^{\dagger} ,\\ \underline{s}_{12}&=\underline{V}_1\underline{D}_{12}\underline{U}_2^{\dagger} ,\\ \underline{s}_{22}&=\underline{V}_2\underline{D}_{22}\underline{U}_2^{\dagger} ,\end{aligned} \tag{A3}$$

where $\underline{D}_{21}$, $\underline{D}_{12}$, and $\underline{D}_{22}$ are complex diagonal matrices, multiplied on the left and on the right by unitary matrices. These diagonal matrices are subject to the constraints

$$\begin{aligned}\underline{D}_{12}^{*}\underline{D}_{12}&=\underline{1}-\underline{D}_{11}^{*}\underline{D}_{11} ,\\ \underline{D}_{21}^{*}\underline{D}_{21}&=\underline{D}_{12}^{*}\underline{D}_{12} ,\\ \underline{D}_{11}^{*}\underline{D}_{11}&=\underline{D}_{22}^{*}\underline{D}_{22} .\end{aligned} \tag{A4}$$

So far, we did not use Eqs. (A1e) and (A1f). These can be cast in the form

$$\begin{aligned}\underline{D}_{21}\underline{D}_{11}^{\dagger}&=-\underline{W}_2^{\dagger}\underline{V}_2\underline{D}_{22}\underline{D}_{12}^{\dagger} ,\\ \underline{D}_{11}^{\dagger}\underline{D}_{12}&=-\underline{D}_{21}^{\dagger}\underline{W}_2^{\dagger}\underline{V}_2\underline{D}_{22} .\end{aligned} \tag{A5}$$

We consider the following two cases: the case where none of the eigenvalues of the diagonal matrices have a modulus equal to 0 or 1, and the case where there exists at least one eigenvalue of these matrices which is equal to 0 or $e^{i\beta}$.

1. Invertible case

If none of the diagonal elements of $\underline{D}_{11}$, $\underline{D}_{12}$, $\underline{D}_{21}$, and $\underline{D}_{22}$ are either 0 or of the form $e^{i\beta}$, with β a real number, then all of these matrices have an inverse. From Eqs. (A3), we can write each diagonal element in the form

$$\begin{aligned}\underline{D}_{11}^{i,i}&=\underline{R}_i^{1/2}e^{i\theta_{11_i}}, \quad \underline{D}_{12}^{i,i}=\underline{T}_i^{1/2}e^{i\theta_{12_i}} ,\\ \underline{D}_{21}^{i,i}&=\underline{T}_i^{1/2}e^{i\theta_{21_i}}, \quad \underline{D}_{22}^{ii}=\underline{R}_i^{1/2}e^{i\theta_{22_i}} .\end{aligned} \tag{A6}$$

Here, none of the elements of the diagonal matrices $\underline{R}^{1/2}$ and $\underline{T}^{1/2}$ can take the value 0 or 1. From Eqs. (A4), we find that $\underline{s}_{21}$ can then be written as

$$\underline{s}_{21}=\underline{V}_2\underline{D}_{21}\underline{U}_1^{\dagger} , \tag{A7}$$

with a relation between the phases of the eigenvalues:

$$\phi_i\equiv\pi-\theta_{11_i}-\theta_{22_i}+\theta_{12_i}+\theta_{21_i}=0 , \tag{A8}$$

for $i=1$ to M. The phase factors can then be absorbed in the unitary matrices $\underline{U}_1$, $\underline{U}_2$, $\underline{V}_1$, and $\underline{V}_2$, by redefining the latter transformations as follows:

$$\begin{aligned}\underline{U}_1&\rightarrow\underline{U}_1e^{i(-\theta_{11_i}/2+\pi/4)} ,\\ \underline{U}_2&\rightarrow\underline{U}_2e^{i(\theta_{12_i}-\theta_{11_i}/2+\pi/4)} ,\\ \underline{V}_1&\rightarrow\underline{V}_1e^{i(\theta_{11_i}/2-\pi/4)} ,\\ \underline{V}_2&\rightarrow\underline{V}_2e^{i(\theta_{22_i}-\theta_{12_i}+\theta_{11_i}/2+-3\pi/4)} .\end{aligned} \tag{A9}$$

With these transformations, we finally obtain the decomposition of Eq. (3.6):

$$\underline{s}_{11}=-i\underline{V}_1\underline{R}^{1/2}\underline{U}_1^\dagger,\quad \underline{s}_{12}=\underline{V}_1\underline{T}^{1/2}\underline{U}_2^\dagger\ ,$$
$$\underline{s}_{21}=\underline{V}_2\underline{T}^{1/2}\underline{U}_1^\dagger,\quad \underline{s}_{22}=-i\underline{V}_2\underline{R}^{1/2}\underline{U}_2^\dagger\ . \tag{A10}$$

2. Zero eigenvalues

If the matrix $\underline{T}$ has a diagonal element equal to 0 (1), then $\underline{R}$ has a corresponding diagonal element equal 1 (0), and one of these matrices has no inverse. As we shall see, this still allows a decomposition of the type (A10).

In the invertible case, Eqs. (A5) allowed us to relate the matrices $\underline{W}_2$ and $\underline{V}_2$ by a unitary, diagonal matrix. We thus study the structure of the matrix $\underline{W}_2^\dagger\underline{V}_2$. For those indices i,j which satisfy $\underline{T}_i\neq 0,1$ and $T_j\neq 0,1$, we have

$$(\underline{W}_2^\dagger\underline{V}_2)_{i,j}=e^{i\phi_i}\delta_{i,j}\ . \tag{A11}$$

For i such that $\underline{T}_i=0$ or $\underline{T}_i=1$, but j as before,

$$(\underline{W}_2^\dagger\underline{V}_2)_{i,j}=0\ . \tag{A12}$$

The matrix $\underline{W}_2^\dagger\underline{V}_2$ thus has the following form:

$$\underline{W}_2^\dagger\underline{V}_2=\begin{pmatrix} e^{i\phi_1} & \cdots & 0 & 0 & \cdots & 0 \\ \vdots & \ddots & \vdots & \vdots & \ddots & \vdots \\ 0 & \cdots & e^{i\phi_M} & 0 & \cdots & 0 \\ & & & & & \\ 0 & \cdots & 0 & & & \\ \vdots & & \vdots & & \underline{U}' & \\ 0 & \cdots & 0 & & & \end{pmatrix}, \tag{A13}$$

with $\underline{U}'$ a unitary matrix. We thus conclude that for the eigenvalues $\underline{T}_i\neq 0,1$, a decomposition of the form (A10) can still be achieved. Eigenvalues with $\underline{T}_i=1$ ($\underline{T}_i=0$) which correspond to perfectly transmitted (reflected) eigenchannels do not require such a decomposition. In the noninvertible case, the decomposition is specified by Eqs. (A2) and (A3), where $\underline{W}_2$ and $\underline{V}_2$ are related by Eq. (A13).

An understanding of the noninvertible case can also be reached by simply considering the limit $\underline{T}_i\to 0$ and $\underline{T}_i\to 1$. Even for an infinitesimal reflection-transmission eigenvalue, the decomposition (A10) is still valid. In this case, the unitary transformation $\underline{U}'$ of Eq. (A13) turns out to be diagonal.

APPENDIX B

Here, we derive formulas that help establish a connection between the present eigenvalue formulation and the approach of Ref. 17 where the noise-power spectrum is expressed in terms of the coefficients of the S matrix.

With $T_i^{\gamma\alpha}$ denoting the eigenvalues of the matrix $\underline{t}_{\gamma\alpha}^\dagger\underline{t}_{\gamma\alpha}$, we first recognize that the sum of the square of the eigenvalues of this matrix can be written as the trace of the matrix $[\underline{t}_{\gamma\alpha}^\dagger\underline{t}_{\gamma\alpha}]^2$. This yields

$$\sum_{i=1}^{\gamma N} T_i^{\gamma\alpha}(1-T_i^{\gamma\alpha})=\mathrm{Tr}[\underline{t}_{\gamma\alpha}^\dagger\underline{t}_{\gamma\alpha}(\underline{1}-\underline{t}_{\gamma,\alpha}^\dagger\underline{t}_{\gamma,\alpha})]\ . \tag{B1}$$

The matrix $[\underline{t}_{\gamma\alpha}^\dagger\underline{t}_{\gamma\alpha}]^2$ is a γN by γN matrix which can be decomposed into $\gamma\times\gamma$ blocks of size $N\times N$ with elements

$$([\underline{t}_{\gamma\alpha}^\dagger\underline{t}_{\gamma\alpha}]^2)_{\beta\delta}=\sum_{\eta=1}^{\gamma}\underline{s}_{\alpha\beta}^\dagger\underline{s}_{\alpha\eta}\underline{s}_{\alpha\eta}^\dagger\underline{s}_{\alpha\delta}\ . \tag{B2}$$

The trace of the matrix $[\underline{t}_{\gamma\alpha}^\dagger\underline{t}_{\gamma\alpha}]^2$ is thus the sum of the traces of all diagonal blocks of this matrix, which gives

$$\sum_{i=1}^{\gamma N} T_i^{\gamma\alpha}(1-T_i^{\gamma\alpha})=\sum_{\eta=1}^{\gamma}\mathrm{Tr}(\underline{s}_{\alpha\eta}\underline{s}_{\alpha\eta}^\dagger)-\sum_{\eta,\delta=1}^{\gamma}\mathrm{Tr}(\underline{s}_{\alpha\eta}\underline{s}_{\alpha\eta}^\dagger\underline{s}_{\alpha\delta}\underline{s}_{\alpha\delta}^\dagger)\ , \tag{B3}$$

where we used the cyclic property of the trace. In a multiterminal structure, the unitarity of the S matrix imposes the relation

$$\sum_{\delta}\underline{s}_{\alpha\delta}\underline{s}_{\alpha\delta}^\dagger=1\ . \tag{B4}$$

Breaking up this sum into two contributions, $\delta=1,2,\ldots,\gamma$ and $\delta=\gamma+1,2,\ldots,P$, we rewrite one of the sums in the second term of Eq. (B3) as $1-\sum_{\eta=\gamma+1}^{P}\mathrm{Tr}(\underline{s}_{\alpha\eta}\underline{s}_{\alpha\eta}^\dagger)$. It then follows that

$$\sum_{i=1}^{\gamma N} T_i^{\gamma\alpha}(1-T_i^{\gamma\alpha})=\sum_{\eta=1}^{\gamma}\sum_{\delta=\gamma+1}^{P}\mathrm{Tr}(\underline{s}_{\alpha\eta}^\dagger\underline{s}_{\alpha\delta}\underline{s}_{\alpha\delta}^\dagger\underline{s}_{\alpha\eta})\ , \tag{B5}$$

which is precisely Eq. (4.4).

The derivation of Eq. (4.7) follows closely the above reasoning. Expressing the sum over eigenvalues in terms of a trace of elements of the S matrix, we find

$$\sum_{i=\gamma N+1}^{PN}\tilde{T}_i^{\gamma\alpha}(1-\tilde{T}_i^{\gamma\alpha})=\sum_{\eta=\gamma+1}^{P}\mathrm{Tr}(\underline{s}_{\alpha\eta}\underline{s}_{\alpha\eta}^\dagger)-\sum_{\eta,\delta=\gamma+1}^{P}\mathrm{Tr}(\underline{s}_{\alpha\eta}\underline{s}_{\alpha\eta}^\dagger\underline{s}_{\alpha\delta}\underline{s}_{\alpha\delta}^\dagger)\ . \tag{B6}$$

Exploiting once again the unitarity of the S matrix, we recover Eq. (4.7).

The matrix $\underline{t}_{\gamma(\alpha+\beta)}^\dagger\underline{t}_{\gamma(\alpha+\beta)}$, which appears in the calculation of correlations between leads α and β, is a γ by γ matrix of blocks of size $N\times N$:

$$(\underline{t}_{\gamma(\alpha+\beta)}^\dagger\underline{t}_{\gamma(\alpha+\beta)})_{\eta\delta}=\underline{s}_{\alpha\eta}^\dagger\underline{s}_{\alpha\delta}+\underline{s}_{\beta\eta}^\dagger\underline{s}_{\beta\delta}\ . \tag{B7}$$

Proceeding as before [Eq. (B1)], the sum over eigenvalues in Eq. (5.11) is written as a trace of this matrix, minus its square. In a first step, we calculate the block elements of the matrix $[\underline{t}_{\gamma(\alpha+\beta)}^\dagger\underline{t}_{\gamma(\alpha+\beta)}]^2$:

$$([\underline{t}_{\gamma(\alpha+\beta)}^\dagger\underline{t}_{\gamma(\alpha+\beta)}]^2)_{\eta\delta}=\sum_{\zeta=1}^{\gamma}(\underline{s}_{\alpha\eta}^\dagger\underline{s}_{\alpha\zeta}\underline{s}_{\alpha\zeta}^\dagger\underline{s}_{\alpha\delta}+\underline{s}_{\beta\eta}^\dagger\underline{s}_{\beta\zeta}\underline{s}_{\beta\zeta}^\dagger\underline{s}_{\beta\delta}+\underline{s}_{\alpha\eta}^\dagger\underline{s}_{\alpha\zeta}\underline{s}_{\beta\zeta}^\dagger\underline{s}_{\beta\delta}+\underline{s}_{\beta\eta}^\dagger\underline{s}_{\beta\zeta}\underline{s}_{\alpha\zeta}^\dagger\underline{s}_{\alpha\zeta})\ . \tag{B8}$$

The sum over eigenvalues now takes the form

$$\sum_{i=1}^{\gamma N} T_i^{\gamma(\alpha+\beta)}(1-T_i^{\gamma(\alpha+\beta)})$$
$$= \sum_{i=1}^{\gamma N} T_i^{\gamma\alpha}(1-T_i^{\gamma\alpha}) + \sum_{i=1}^{\gamma N} T_i^{\gamma\beta}(1-T_i^{\gamma\beta})$$
$$-2\sum_{\eta=1}^{\gamma}\sum_{\delta=\gamma+1}^{P} \mathrm{Tr}(\underline{s}_{\alpha\eta}\underline{s}_{\beta\eta}^{\dagger}\underline{s}_{\beta\delta}\underline{s}_{\alpha\delta}^{\dagger}) , \quad \text{(B9)}$$

where we recognize contributions of the form (B3) in the two first terms on the right-hand side. For the last term of Eq. (B9), we have used the identity

$$\sum_{\delta} \underline{s}_{\alpha\delta}\underline{s}_{\beta\delta}^{\dagger} = 0, \quad \alpha \neq \beta . \quad \text{(B10)}$$

The calculation of the sum over the eigenvalues of the matrix $\underline{\tilde{t}}_{\gamma(\alpha+\beta)}\underline{\tilde{t}}_{\gamma(\alpha+\beta)}^{\dagger}$ is carried out along similar lines. Here, we give the result

$$\sum_{i=1}^{\gamma N} \tilde{T}_i^{\gamma(\alpha+\beta)}(1-\tilde{T}_i^{\gamma(\alpha+\beta)})$$
$$= \sum_{i=1}^{\gamma N} \tilde{T}_i^{\gamma\alpha}(1-\tilde{T}_i^{\gamma\alpha}) + \sum_{i=\gamma+1}^{\gamma N} \tilde{T}_i^{\gamma\beta}(1-\tilde{T}_i^{\gamma\beta})$$
$$-2\sum_{\eta=1}^{\gamma}\sum_{\delta=\gamma+1}^{P} \mathrm{Tr}(\underline{s}_{\alpha\eta}\underline{s}_{\beta\eta}^{\dagger}\underline{s}_{\beta\delta}\underline{s}_{\alpha\delta}^{\dagger}) . \quad \text{(B11)}$$

[1] *Nanostructure Physics and Fabrication,* edited by W. P. Kirk and M. Reed (Academic, New York, 1989).

[2] See, for example, *The Quantum Hall Effect,* edited by R. Prange and S. M. Girvin (Springer-Verlag, New York, 1987).

[3] B. J. van Wees *et al.*, Phys. Rev. Lett. **60**, 848 (1988).

[4] S. Washburn and R. Webb, Adv. Phys. **35**, 375 (1986).

[5] R. Landauer, in *Analogies in Optics and Micro-Electronics,* edited by W. van Haeringen and D. Lenstra (Kluwer Academic, Dordrecht, 1990), p. 243.

[6] J. R. Pierce, Bell Syst. Technol. J. **27**, 15 (1948).

[7] P. Dutta and P. M. Horn, Rev. Mod. Phys. **53**, 497 (1981); M. B. Weissman, *ibid.* **60**, 537 (1988).

[8] S. Feng, P. A. Lee, and A. D. Stone, Phys. Rev. Lett. **56**, 1960 (1986).

[9] D. H. Cobden, N. K. Patel, M. Pepper, D. A. Richtie, J. E. F. Frost, and G. A. C. Jones (unpublished).

[10] Y. P. Li, A. Zaslavsky, D. C. Tsui, M. Santos, and M. Shayegan, Phys. Rev. B **41**, 8388 (1990).

[11] Y. P. Li, D. C. Tsui, J. J. Heremans, J. A. Simmons, and G. W. Weimann, Appl. Phys. Lett. **57**, 774 (1990).

[12] A. J. Kil, R. J. J. Zijlstra, M. F. H. Schuurmans, and J. P. Andre, Phys. Rev. B **41**, 5169 (1990).

[13] S. Washburn, R. J. Haug, K. Y. Lee, and J. M. Hong (unpublished).

[14] R. Landauer, Physica D **38**, 226 (1987).

[15] G. B. Lesovik, Pis'ma Zh. Eksp. Teor. Fiz. **49**, 594 (1989) [JETP Lett. **49**, 683 (1989)].

[16] B. Yurke and G. P. Kochlanski, Phys. Rev. B **41**, 8141 (1990).

[17] M. Büttiker, Phys. Rev. Lett. **65**, 2901 (1990); in *Granular Nanoelectronics, NATO Advanced Study Institute Series B: Physics,* edited by D. K. Ferry (Plenum, New York, 1991).

[18] L. V. Keldysh, Zh. Eksp. Teor. Fiz. **47**, 1515 (1964) [Sov. Phys. JETP **20**, 1018 (1965)].

[19] L. Y. Chen, G. Levine, J. Yang, and C. S. Ting (unpublished); C. W. J. Beenakker and H. van Houten (unpublished).

[20] Y. P. Li, A. Zaslavsky, D. C. Tsui, M. Santos, and M. Shayegan, in *Resonant Tunneling in Semiconductors: Physics and Applications,* edited by L. L. Chang, E. E. Mendez, and C. Tejedor (Plenum, New York, 1991).

[21] R. Landauer and Th. Martin, Physica B (to be published).

[22] B. J. Thompson, RCA Rev. **2**, 269 (1940); D. O. North, *ibid.* **4**, 441 (1940); A. J. Rack, Bell Syst. Technol. J. **17**, 592 (1938).

[23] M. Büttiker and R. Landauer, Phys. Rev. Lett. **49**, 1739 (1982); M. Büttiker, in *Electronic Properties of Multilayers and Low-Dimensional Semiconductors Structures,* edited by J. M. Chamberlain *et al.* (Plenum, New York, 1990); R. Landauer, Ber. Bunsenges. **95**, 404 (1991).

[24] K. W. H. Stevens, J. Phys. C **20**, 5791 (1987); C. E. Shannon, Proc. IRE **37**, 10 (1949).

[25] See, for example, S. O. Rice, in *Noise and Stochastic Processes,* edited by N. Wax (Dover, New York, 1954), p. 133.

[26] M. Büttiker, IBM J. Res. Develop. **32**, 317 (1988).

[27] P. A. Mello, P. Peyreyra, and N. Kumar, Ann. Phys. **181**, 290 (1988); P. A. Mello and J. L. Pichard, J. Phys. I **1**, 493 (1991).

[28] M. Büttiker and Th. Martin (unpublished).

[29] K. v. Klitzing, G. Dorda, and M. Pepper, Phys. Rev. Lett. **45**, 495 (1980).

[30] S. Washburn, A. B. Fowler, H. Schmid, and D. Kern, Phys. Rev. Lett. **61**, 2801 (1988); R. J. Haug, A. H. MacDonald, P. Streda, and K. v. Klitzing, *ibid.* **61**, 2797 (1988).

[31] J. K. Jain and S. A. Kivelson, Phys. Rev. Lett. **60**, 1542 (1988); Phys. Rev. B **37**, 4276 (1988); P. Streda, J. Kucera, and A. H. MacDonald, Phys. Rev. Lett. **59**, 1973 (1987).

[32] M. Büttiker, Phys. Rev. Lett. **57**, 1761 (1986); Phys. Rev. B **38**, 9375 (1988).

[33] R. Hanbury Brown and R. Q. Twiss, Nature **177**, 27 (1956).

[34] R. Hanbury Brown and R. Q. Twiss, Proc. R. Soc. London Ser. A **242**, 300 (1957); **243**, 291 (1957).

[35] S. Murphy (private communication).

[36] M. Büttiker, Physica B **175**, 199 (1991).

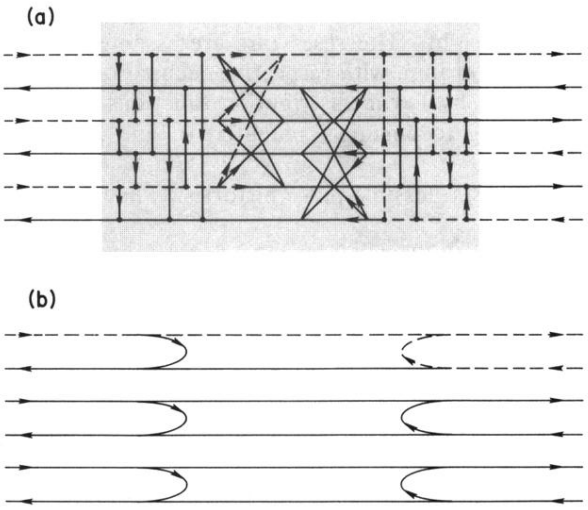

FIG. 2. Invertible case. (a) Schematic representation of mixing between incident and outgoing channels in the sample. The sample is connected on both sides with three propagating channels. Vertical lines represent the transfer from incoming channels to outgoing channels. (b) In the representation of channels specified by the transformation of Eq. (3.6), the sample simply reduces to a set of decoupled one-dimensional channels.

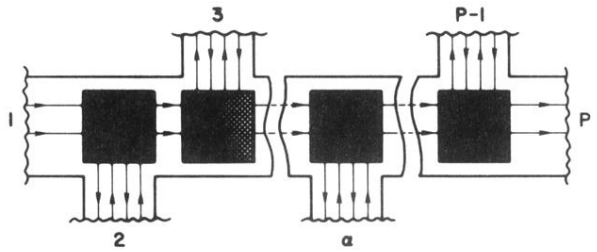

FIG. 4. Multiterminal sample: each lead carries two channels, and the arrows specify the direction of electron motion, as constrained by Fermi blocking at zero temperature. The shaded boxes represent the mixing between channels (the fact that the spatial sequence of the reservoirs agrees with the ordering of the chemical potentials is only for simplicity, and not part of the argument).